Supporting Information

A Near Infrared Optical Nanosensor for Measuring Aerobic Respiration in Microbial Systems

Samuel C. Saccomano[a], Kevin J. Cash[a,b]

Chemical and Biological Engineering Department, Colorado School of Mines, Golden, Colorado 80401, United States

Quantitative Biosciences and Engineering, Colorado School of Mines, Golden, Colorado, 80401, United States

**Figure S1.** The nanosensors are composed of an oxygen-sensitive dye (PtOEPK) and oxygen-insensitive dye (DiD) encapsulated within a polymer matrix. In the absence of oxygen the PtOEPK emits a luminescent signal when excited by a photon. However, in the presence of oxygen the dye is quenched and the excess energy dissipated into non-radiative heat. As the oxygen gets progressively lower in concentration, the signal from the PtOEPK dye increases while the signal from the DiD dye does not change. Created with BioRender.com.
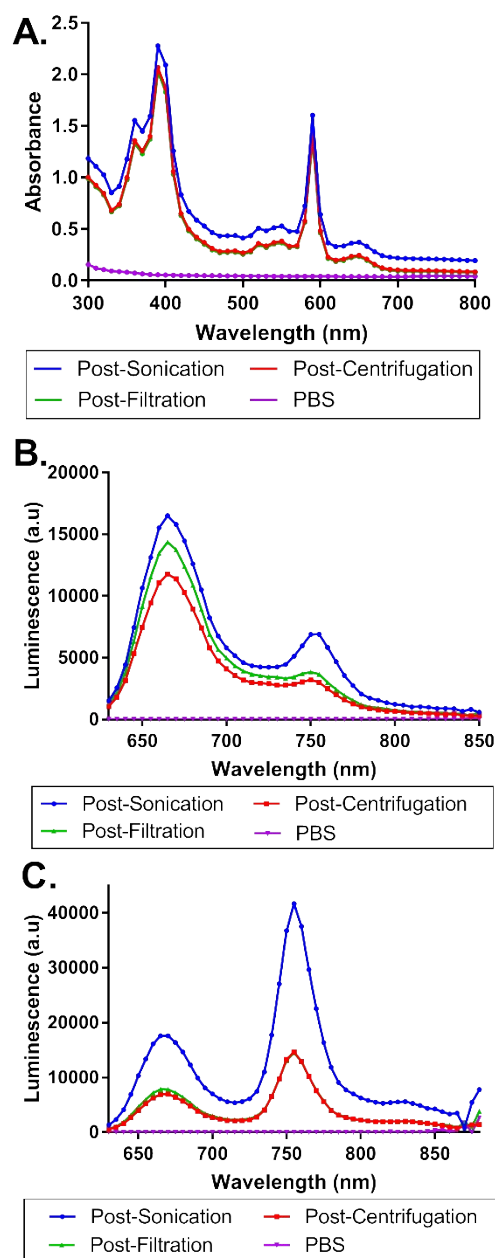
**Figure S2.** To estimate potential losses during the fabrication process, a batch of nanosensors was measured directly after a sonication step, after a centrifugation step, and after our standard filtration step to compare where the most significant losses in the process were observed. **A.** Absorbance measurements showed roughly a 10-15% loss from the initial 2.3 mg/mL of input material when insoluble particles were centrifuged out. Conversely, filtration showed no drop in signal compared to centrifuged samples, indicating that the losses in the process are primarily from polymer materials and aggregates which were not solubilized. Luminescence measurements **B.** in the presence of oxygen and **C.** in the absence of oxygen also confirm this result though the loss in signal was greater compared to absorbance (highlighting potential issues with using luminescence to judge particle loss).

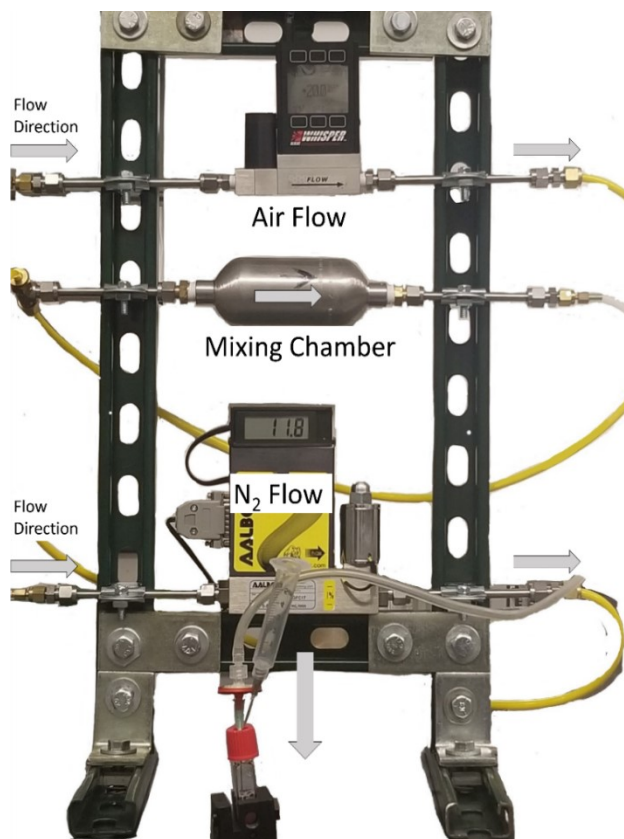**Figure S3.** Diagram showing oxygen calibration setup for $O_2$-sensitive nanosensors. $N_2$ and Air gas streams are controlled by mass flow controllers and mixed within a stainless-steel mixing chamber before bubbling into the nanosensor solution in the cuvette.
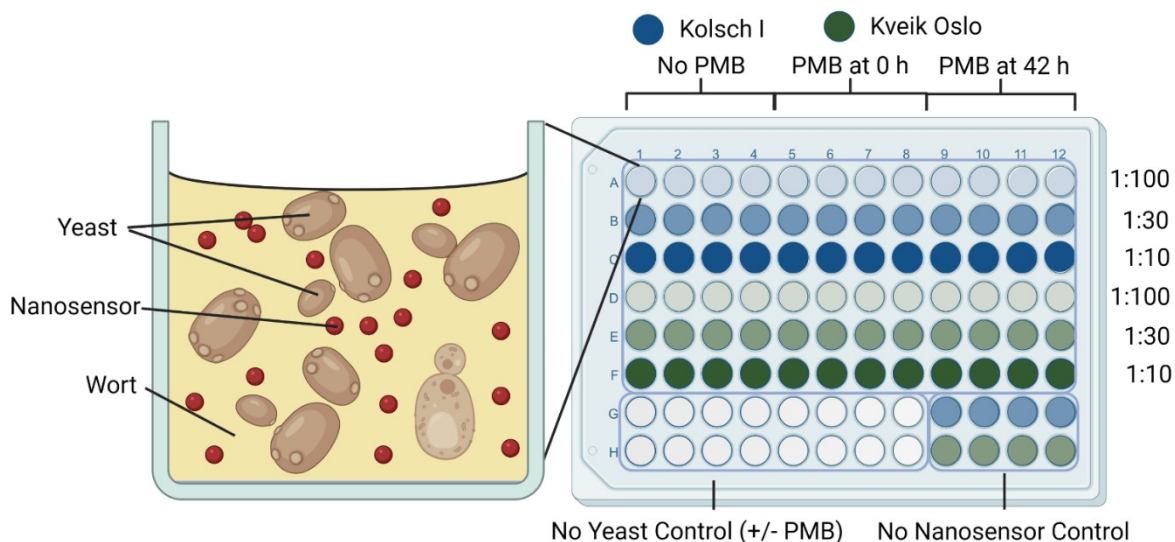
**Figure S4.** The basic contents of each well 200 µL of a mixture containing the yeast, the ratiometric oxygen nanosensors and the wort media. The plate layout for this experiment tested 18 different conditions across 3 dilutions of yeast, 2 strains of yeast and 3 antimicrobial exposure conditions. Each condition was replicated across 4 replicate wells. No yeast controls with and without the PMB were included with 8 replicate wells of each. No nanosensor controls of the 1:30 dilution of each strain was test in quadruplicate wells. Not to scale. Created in BioRender.com.

**Figure S5.** The raw luminescence spectra for the oxygen nanosensors containing PtOEPK dye and DiD dye when measured at different concentrations of oxygen. Luminescence of the PtOEPK increases as oxygen concentrations decrease from atmospheric (6.65 mg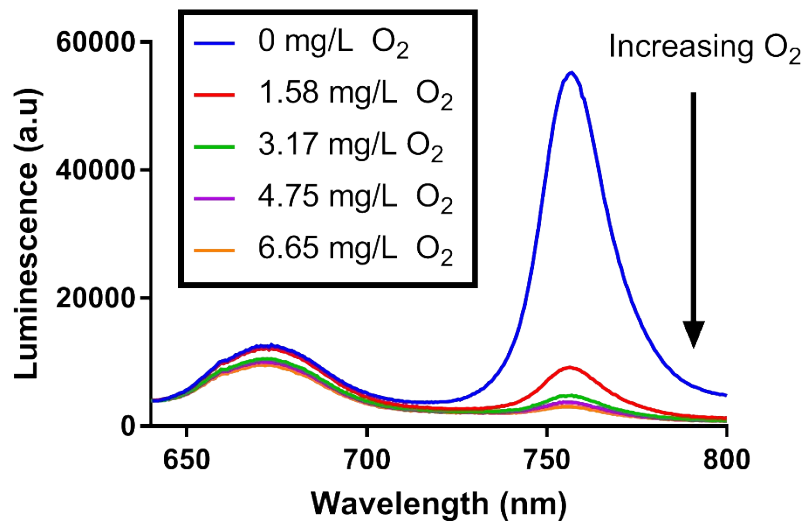/L) conditions to anoxic (0 mg/L) conditions. This dataset represents the data in Figure 1 before normalization to the peak DiD luminescence value.

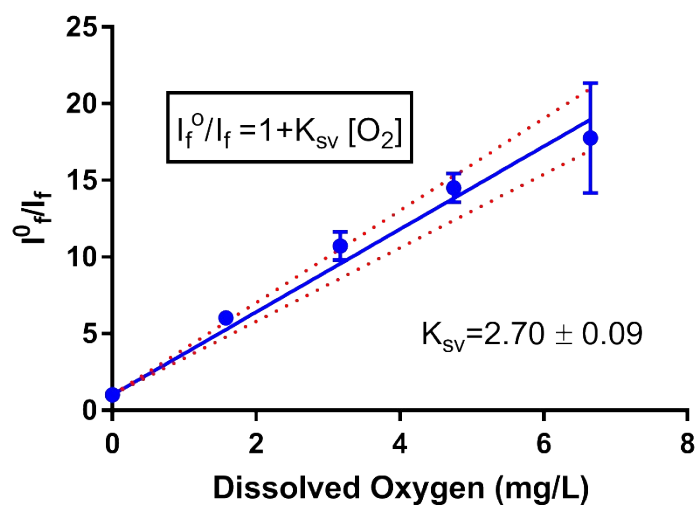**Figure S6.** The Stern Volmer calibration plot for PtOEPK luminescence at varying concentration of oxygen generated by air and nitrogen bubbling. The dye show a highly linear correlation and great sensitivity from anoxic (0 mg/L) to atmospheric (6.65 mg/L) conditions (n=3). This figure represents the same experimental data as Figure 2 except using only the PtOEPK signal instead of the ratiometric signal.

**A.**

$I^0_f/I_f$ vs Dissolved Oxygen (mg/L)

$K_{sv}=2.70 \pm 0.03$

**B.**

Ratiometric Signal vs Dissolved Oxygen (mg/L)

$K_{sv}=2.35 \pm 0.04$

**Figure S7.** The **A.** Stern Volmer Plot and **B.** Pseudo-Stern Volmer calibration plots for the oxygen-sensitive nanosensor when tested in 0.39 mg/L increments within the 0-1.58 mg/L range by air and nitrogen bubbling. The sensors show even greater sensitivity and linearity than the wider oxygen concentration range (n=3). Note that these experiments were performed on a separate batch of nanosensors which may account for any of the discrepancies in the $K_{sv}$ or $K_{psv}$ values.

**Figure S8.** The nanosensors are continually cycled through oxygenated and deoxygenated state to show reversibility of the PtOEPK dye. Over 5 cycles the dye retains its original brightness with great consistency across nanosensor batches (n=3). This figure represents the same experimental data as Figure 3 except using only the PtOEPK signal instead of the ratiometric signal. Where not visible, error bars are smaller than data points.
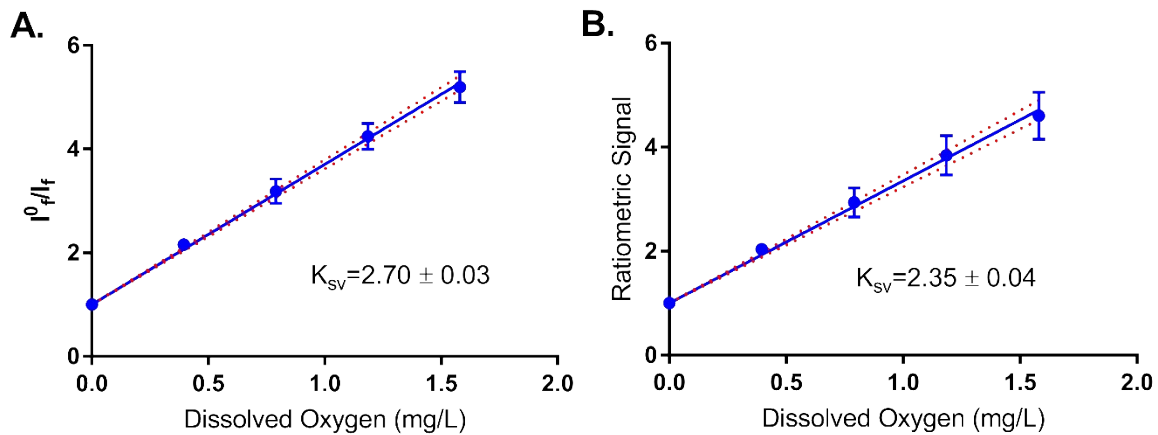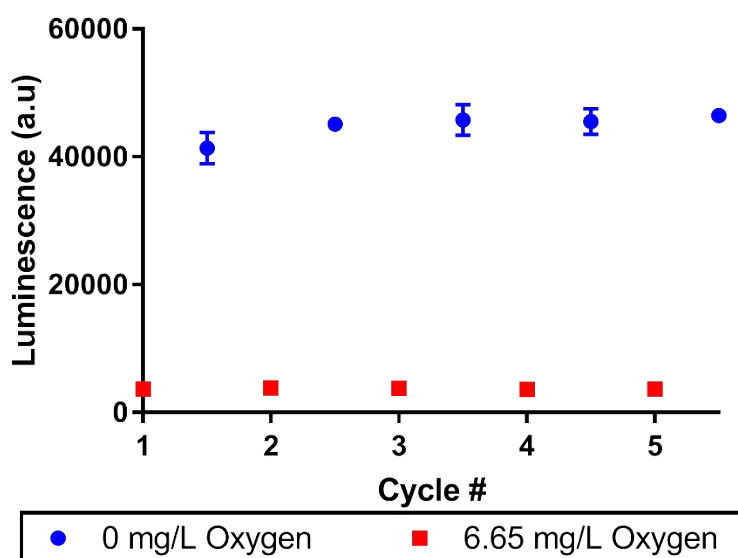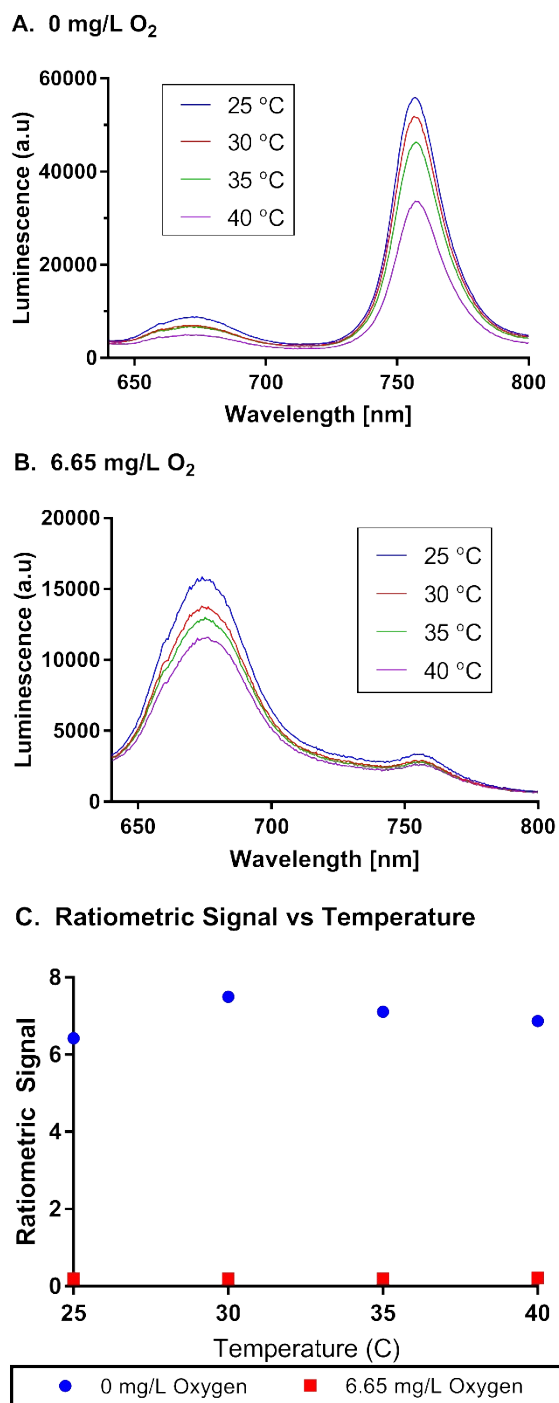
A. 0 mg/L $O_2$



B. 6.65 mg/L $O_2$



C. Ratiometric Signal vs Temperature



**Figure S9.** Temperature dependent emission spectra for Near-Infrared nanosensors. **A.** Emission spectra at 0 mg/L (anoxic) dissolved $O_2$ concentration and **B.** 6.65 mg/L (atmospheric) $O_2$ concentration from 25° to 40° Celsius. Both dyes show dependence on temperature with significant loss of signal at higher temperatures. **C.** The ratiometric signal of the two dyes shows consistent measurements from 25° to 40° C.
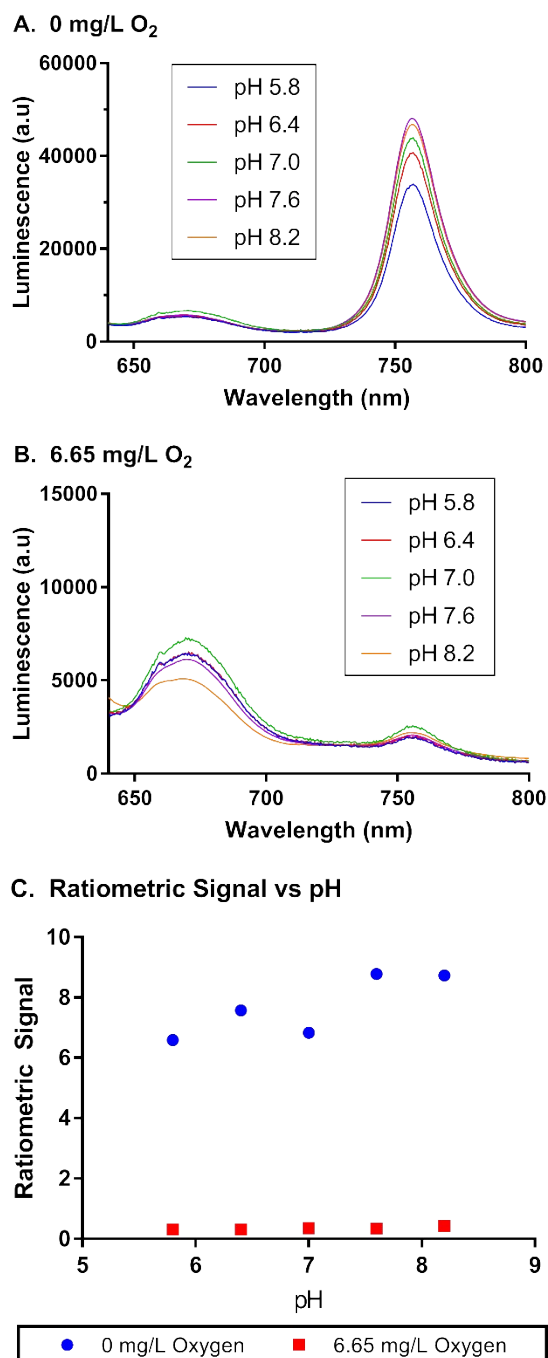
**Figure S10.** pH-dependent emission spectra for Near-IR nanosensors. Emission spectra at **A.** 0 mg/L $O_2$ (anoxic) and **B.** 6.65 mg/L $O_2$ (atmospheric) for pH ranging from 5.8 to 8.2. $O_2$-Sensitive dye shows consistent fluorescence for pH range 6.4 to 8.2, but loss of signal was observed at pH 5.8. Reference dye was only affected at pH 8.2 with consistent measurements for pH 5.8 to 7.6. **C.** The ratiometric signal of the $O_2$-sensitive dye and the reference dye is constant at pH 5.8 to 7.0 and increased at pH 7.6 and 8.2.

**A. Raw PtOEPK Signal**
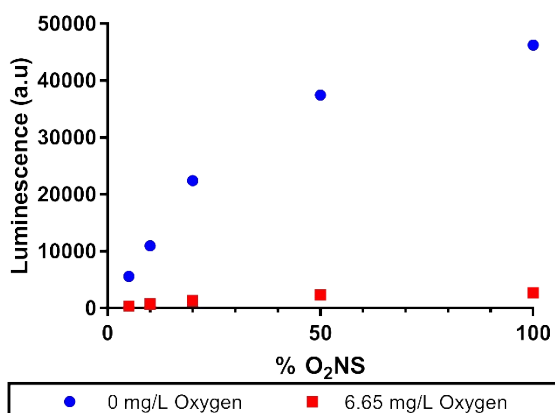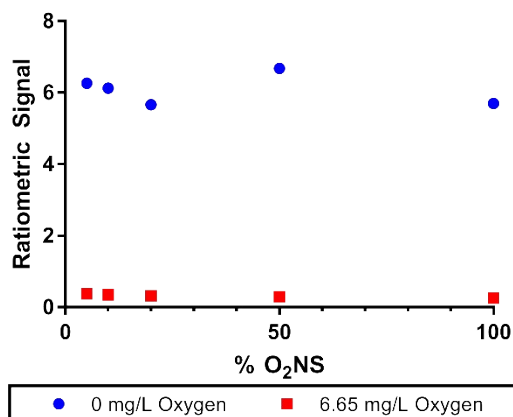


**B. Ratiometric Signal**



**Figure S11.** Concentration dependence of Near-Infrared $O_2$ nanosensors with respect to luminescence **A.** Dilution of nanosensors does not show a linear decrease in signal of the PtOEPK dye at 0 mg/L or 6.65 mg/L $O_2$ **B.** The signal ratio of the PtOEPK and DiD dyes show consistency at any dilution indicating that both dyes decrease in signal at the same rate as nanosensor concentration is diluted.
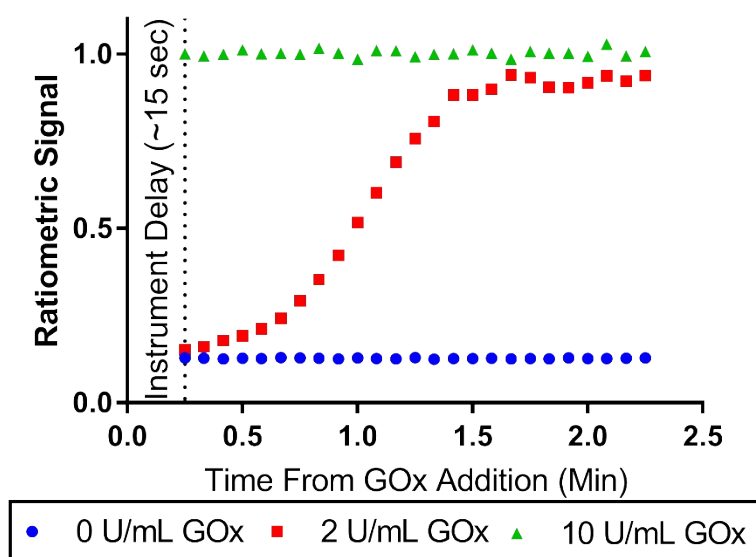
**Figure S12.** The response time of the nanosensors is tested through the rapid depletion of oxygen via glucose and glucose oxidase. With no glucose oxidase, the oxygen level stays constant. At a low glucose oxidase concentration (2 U/mL), the signal changes slowly as the glucose oxidase depletes oxygen from the sample at a slow rate. At a high glucose oxidase concentration (10 U/mL), oxygen depletion is no longer the limiting factor and the sensors respond faster than we can measure with the instrumentation used. This shows that as an upper bound, the sensors respond fully in less than 15 seconds though the actual response time may be much faster.
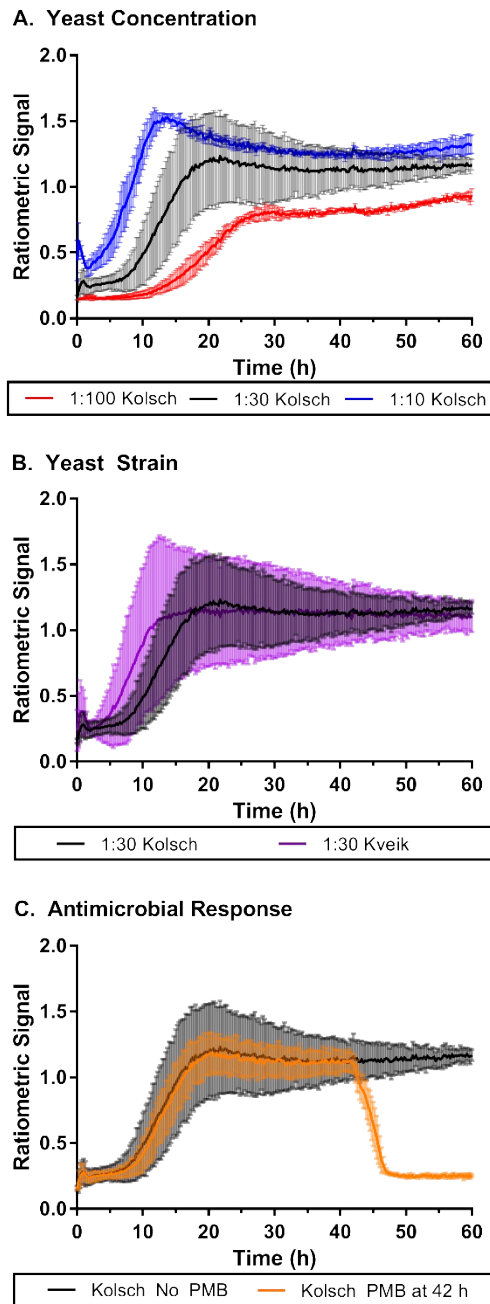
**Figure S13.** Oxygen nanosensor response in yeast growth assay (same as Figure 4) with error bars for the standard deviation of n=4 replicates. **A.** Yeast diluted at varying cell concentrations show faster oxygen consumption and higher equilibrium oxygen concentrations for more concentrated samples of yeast. **B.** Kolsch and Kveik strains of yeast show similar oxygen consumption behavior though the Kveik strain metabolized oxygen faster potentially due to high cell counts. **C.** Potassium Metabisulfite when added at 42 h from inoculation causes an immediate decrease in oxygen metabolism in the samples.
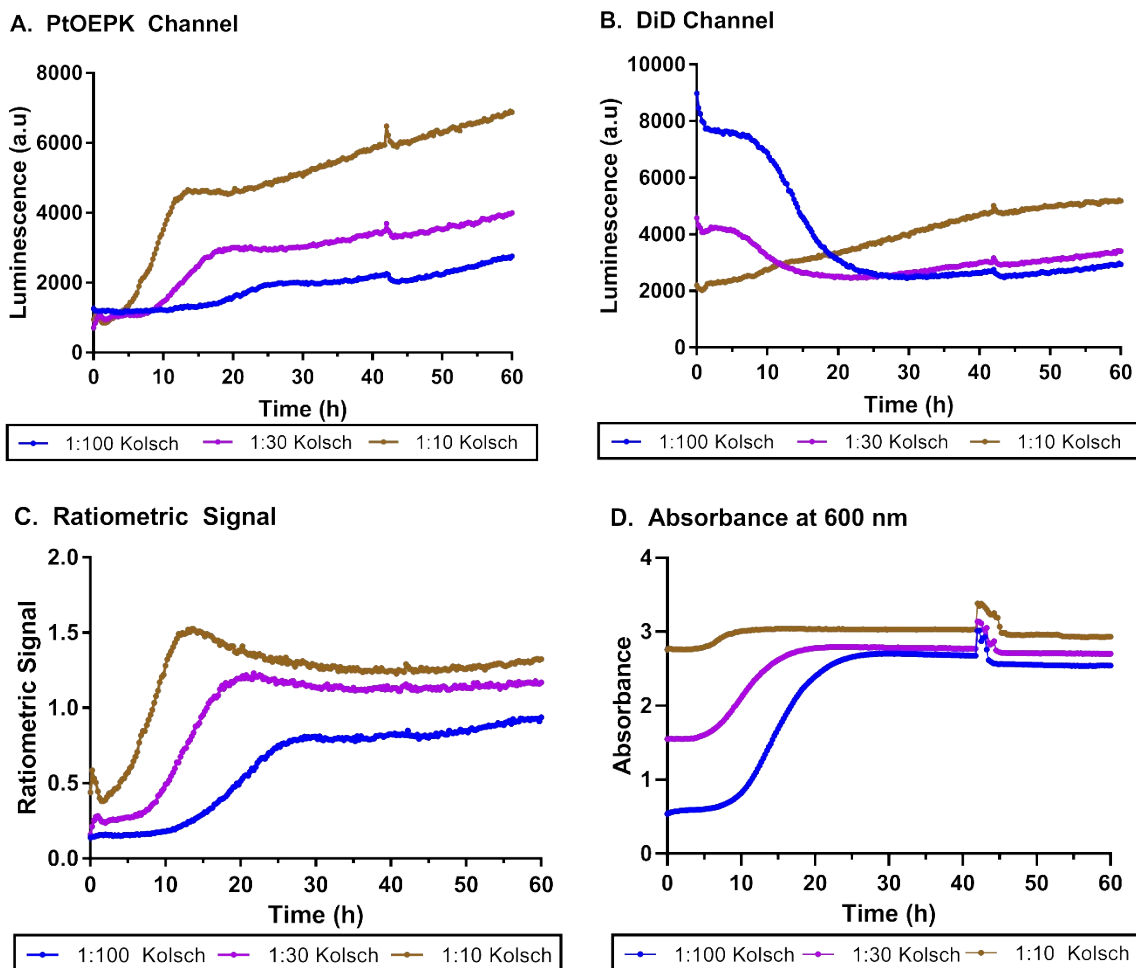
**A. PtOEPK Channel**



**B. DiD Channel**



**C. Ratiometric Signal**



**D. Absorbance at 600 nm**



**Figure S14.** The ratiometric plot is able to deconvolute the oxygen behavior by taking the ratio of the two dye luminescence signals. **A.** The PtOEPK channel (757 nm emission) and the **B.** DiD channel (675nm emission) show artifacts such as signal drift when plotted individually. **C.** The ratiometric signal makes sense of the data to show a clear trend in oxygen concentration changes. **D.** Absorbance of the yeast as they grow (in addition to other factors) may contribute to behavior of the signal of the two dyes.
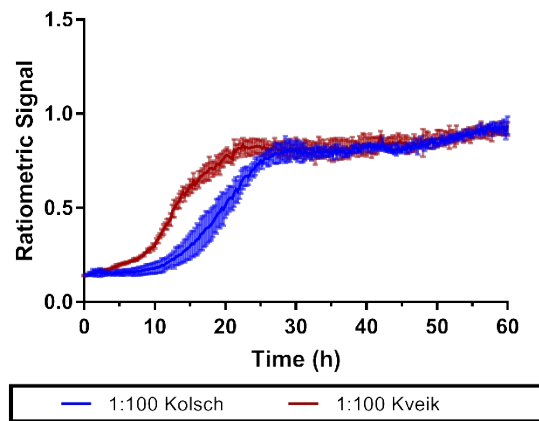
**A. 1:100 Dilution**
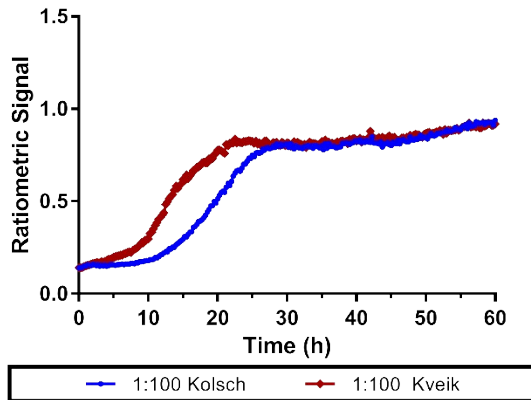


**B. 1:10 Dilution**
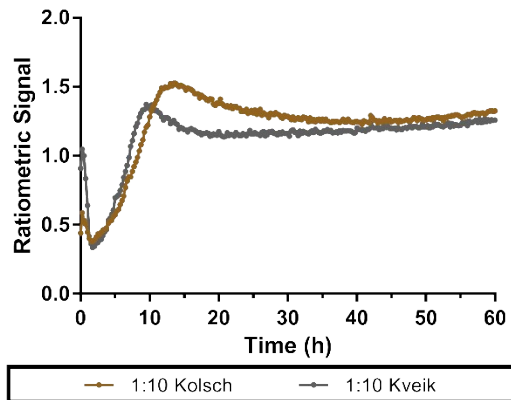


**C. 1:100 Dilution - Error Bars**
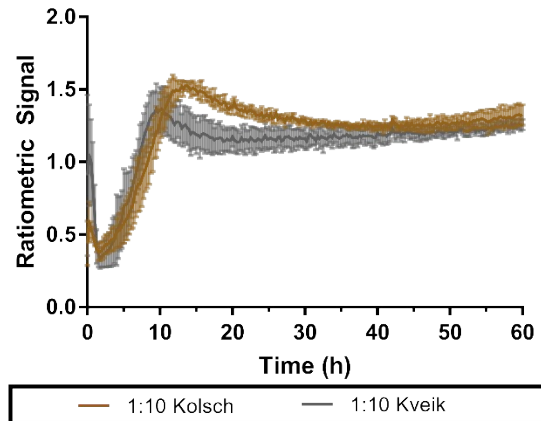


**D. 1:10 Dilution - Error Bars**



**Figure S15.** Comparison of Kolsch and Kveik strains at **A.** 1:100 yeast dilution and **B.** 1:10 yeast dilution over growth period. Kveik shows faster oxygen consumption at lower cell concentrations, but at higher cell concentrations the Kolsch reached a lower overall oxygen concentration before reaching equilibrium oxygen concentration. **C.** and **D.** represent each of the previous graphs with addition of errors for n=4 replicates at each datapoint.
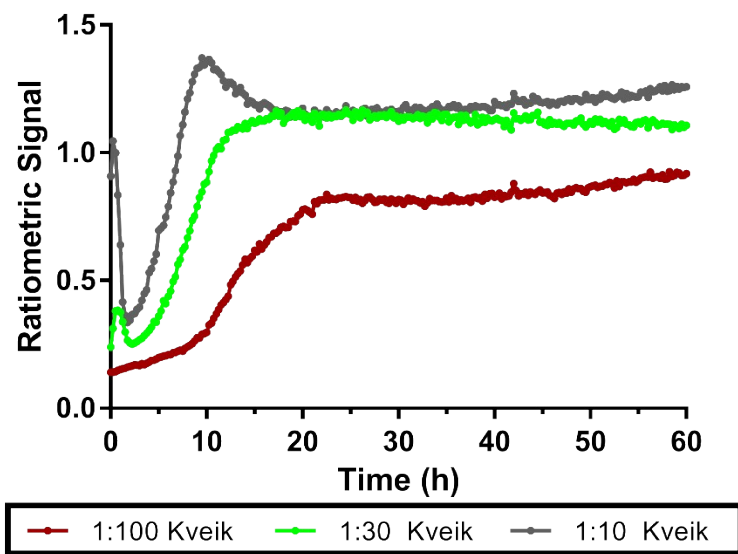
**Figure S16.** Yeast dilution concentrations for the Kveik Strain show similar trends to the Kolsch strain exhibiting higher oxygen metabolism at higher cell concentration.
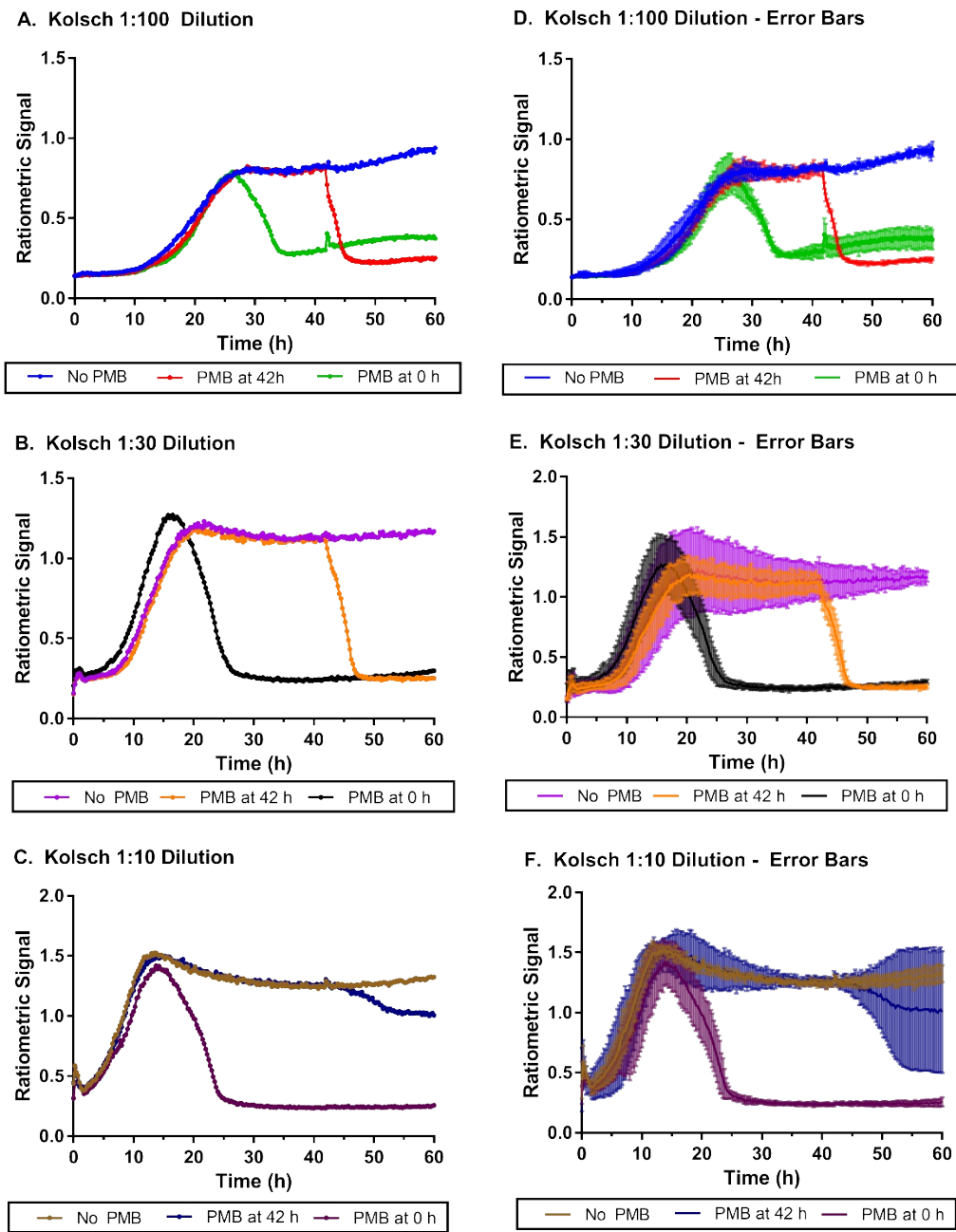
**Figure S17.** Yeast oxygen metabolism in Kolsch strain is affected greatly by the addition of potassium metabisulfite when added at 0 h and 42 h after inoculation. **A.** 1:100 yeast dilution **B.** 1;30 yeast dilution and **C.** 1:10 yeast dilutions show very similar trends. Yeast with PMB added initially has a delay period before yeast metabolism is affected while samples given PMB at 42 h saw immediate increase in oxygen concentration. Only the 1:10 yeast dilution did not return to initial oxygen levels. Panels **D.**, **E.**, and **F.** are that same as panels **A.**, **B.**, and **C.** respectively with the addition of error bars representing the standard deviation for n=4 replicates.
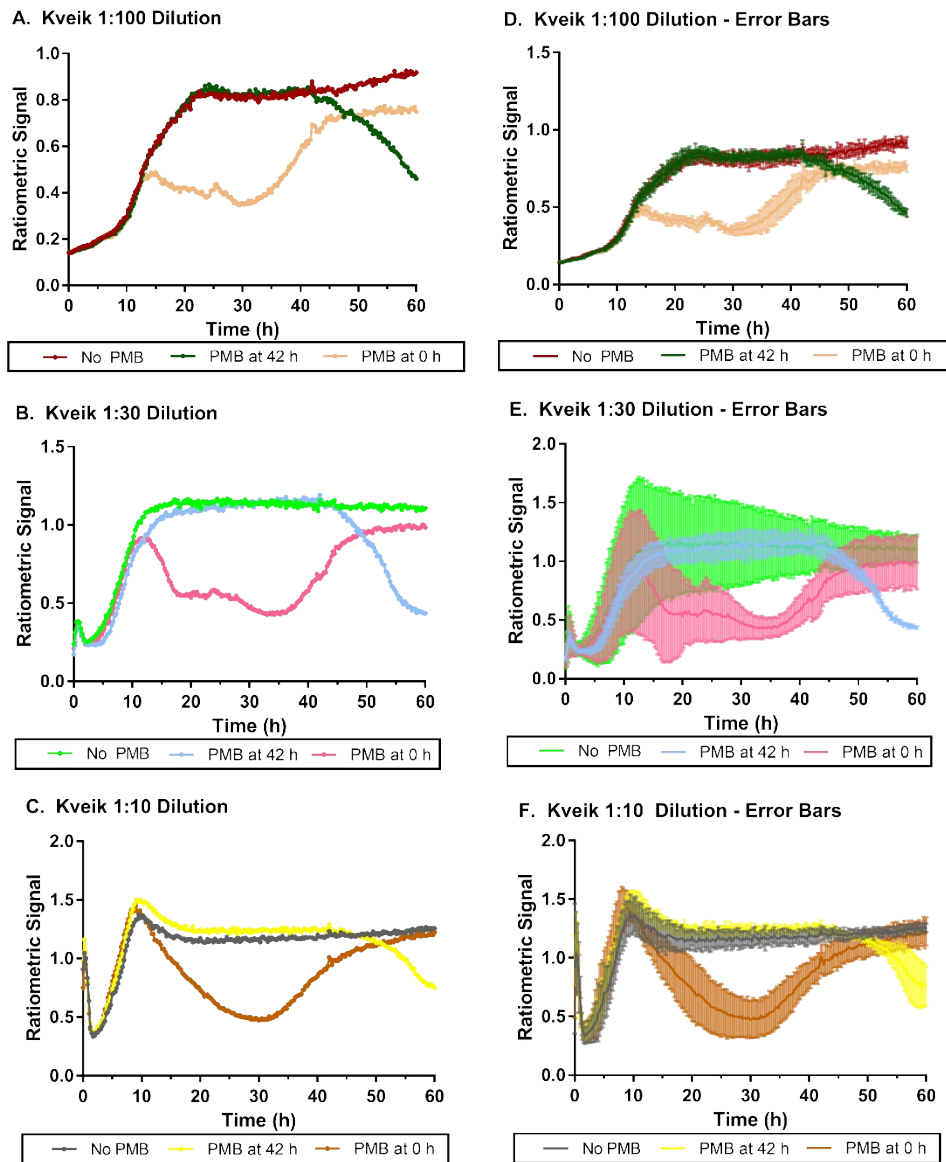
**Figure S18.** The Kveik strain of yeast shows better tolerance of potassium metabisulfite as compared to Kolsch Strain. At **A.** 1:100 yeast dilution **B.** 1:30 yeast dilution and **C.** 1:10 yeast dilution samples with PMB initially added show a similar delayed response in slowed metabolism, however, there is a "recovery period" between 30-40 h where the yeast re-establish strong oxygen consumption rates. Yeast samples with PMB added at 42 h showed a slower increase in oxygen concentration and did not reach atmospheric levels 18 h after addition of the PMB. Panels **D.**, **E.**, and **F.** are that same as panels **A.**, **B.** and **C.** respectively with the addition of error bars representing the standard deviation for n=4 replicates.
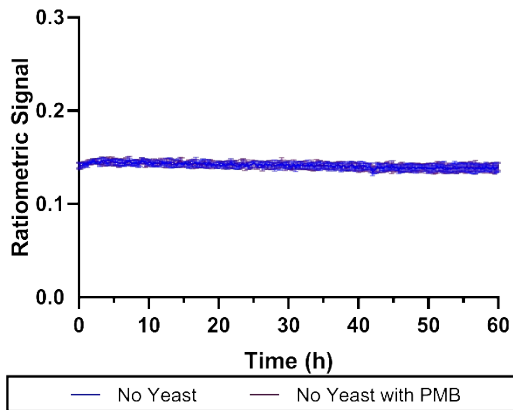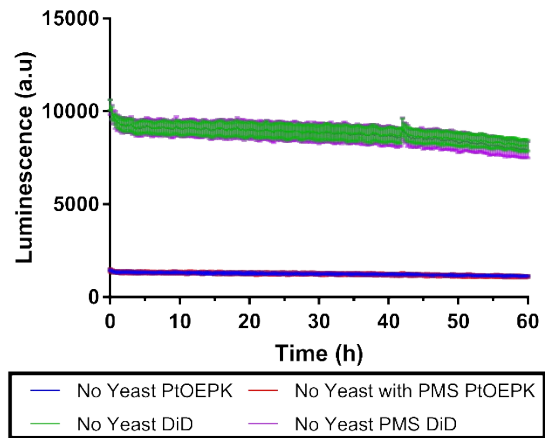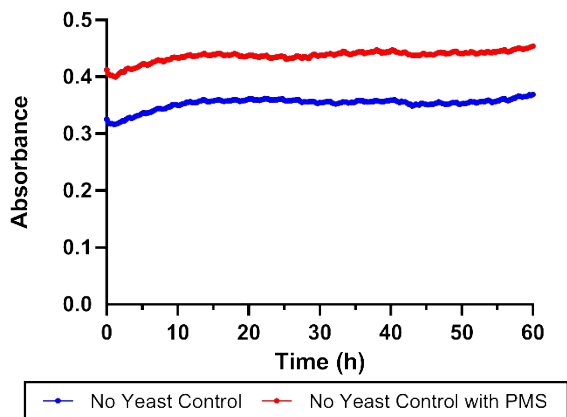
**A. No Yeast - Ratiometric Signal**

**B. No Yeast - Both Dye Channels**

**C. No Yeast - Absorbance at 600 nm**
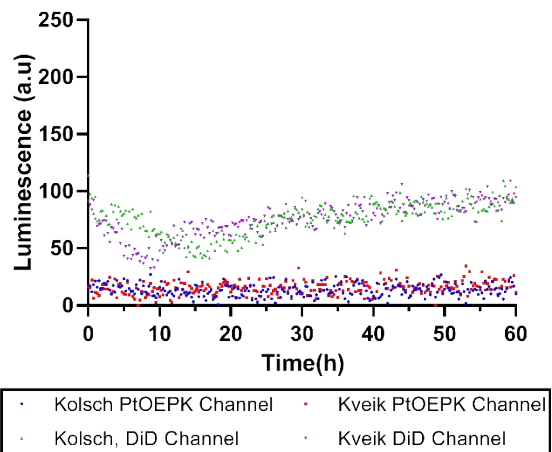
**D. No Nanosensor - Both Dye Channels**

**Figure S19.** Controls show expected behaviors in luminescence and absorbance data. **A.** Ratiometric signal of the nanosensor in the absence of yeast stays constant as oxygen concentration stays constant. **B.** PtOEPK and DiD dyes show minimal signal drift over the 60 h period. Datasets A and B are each shown with errors of n=8 and n=4 replicates respectively **C.** Absorbance data shows no contamination or growth in no yeast control wells. **D.** No nanosensor controls show minimal background autofluorescence at the overlapping emission wavelength with PtOEPK and DiD dyes for both yeast strains.
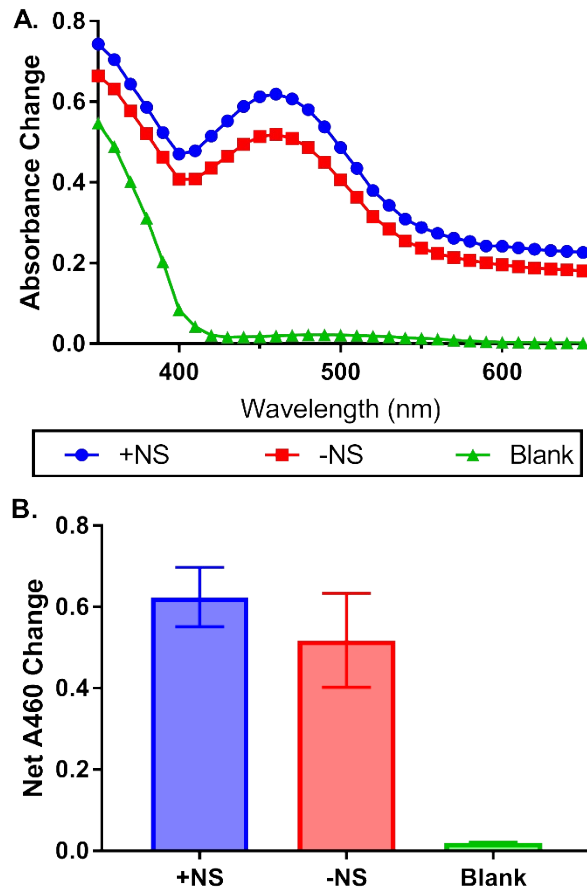
**Figure S20.** Yeast cells exposed to nanosensor for 48 h do not show significant toxicity compared to cells without nanosensor as tested by a CCK-8 metabolic assay (n=3). **A.** The spectra calculated from the net change in absorbance after incubating the cells for 24 h with CCK-8 showed that cell activity in the samples with nanosensor was slightly higher than that of the cells without nanosensor. **B.** Upon investigation of the A460 we found that the signal of the two samples was within error. A t-test was performed to compare the two data sets which resulted in a p-value of 0.067.
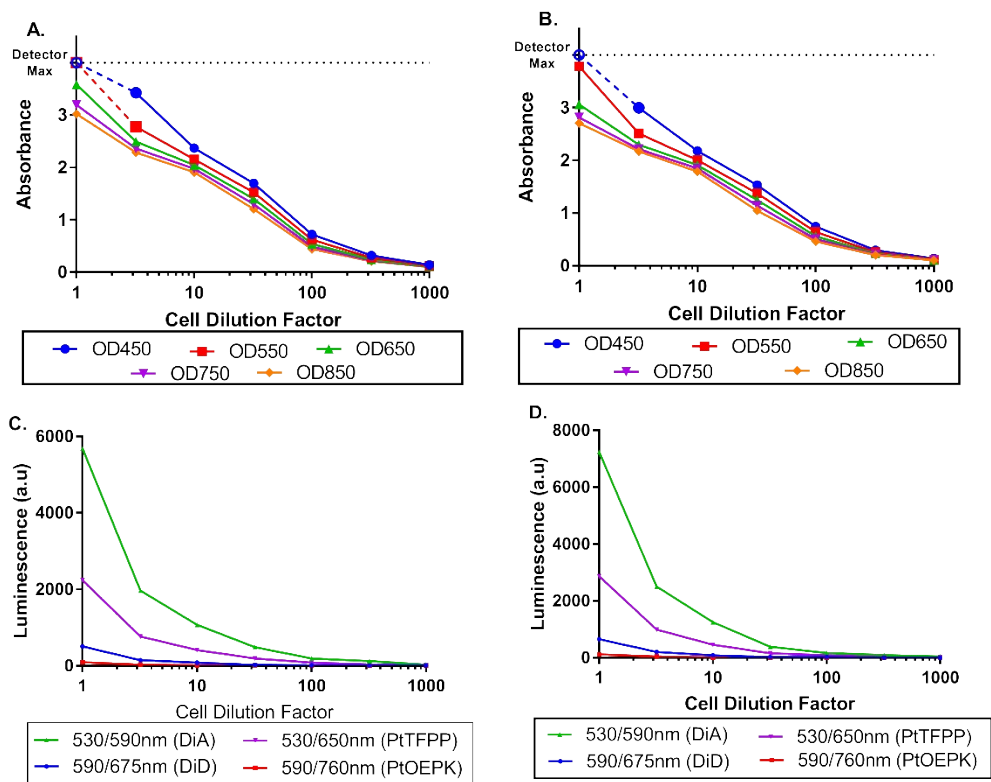
**Figure S21.** Yeast cell stocks show significant levels of absorbance and autoluminescence at high concentrations of cells in wort (versus PBS diluted samples) as well as low emission and excitation wavelengths. The absorbance for **A.** Kolsch and **B.** Kveik yeast show that while absorbance at NIR wavelengths is still significant, it is much less than that of blue-shifted wavelengths where several samples maxed out the detector limit. Autoluminescence for the **C.** Kolsch and **D.** Kveik strains were compared at wavelengths for our NIR nanosensors as compared to previously used oxygen sensors that included a PtTFPP (650nm emission) and DiA (590 emission)[18] dye combination showing a significant decrease in autoluminescence due to the higher excitation wavelength (530nm vs 590nm) and emission wavelength even at 10x cell dilution.